0273–2289/87/1401–0049$04.80

Mixed Enzymic Reaction–Internal Diffusion Kinetics of Nonuniformly Distributed Immobilized Enzymes

The System Agarose-Micrococcal Endonuclease

J. M. GUISAN, J. SERRANO, F. V. MELO, AND A. BALLESTEROS*

Instituto de Catálisis, CSIC, 28006 Madrid, Spain

Received June 21, 1986; Accepted July 17, 1986

ABSTRACT

Two types of (CNBr-activated) Agarose-staphylococcal endonuclease derivatives have been prepared, one with the enzyme uniformly distributed in the support, and the other with the enzyme preferentially bound in the most external part of the support particles; the latter were obtained using agarose of very small pores and a high degree of activation. Quantitative enzyme distribution has been determined by scanning fluorescence microscopy. With these insoluble enzyme derivatives, a kinetic study for the hydrolysis of a mononucleotide has been carried out. A simple theoretical model for nonuniformly distributed insoluble enzyme derivatives, which considers only the case of mixed enzymic reaction–internal diffusion kinetics, is proposed. The experimental data agree very well with the predictions of the model.

Index Entries: CNBr-activated agarose; staphylococcal nuclease; heterogeneously distributed insolubilized enzymes, preparation of; inhomogeneously distributed insolubilized enzymes, preparation of; insolubilized enzymes, preparation of inhomogeneously distributed; fluorescence, determination of enzyme distribution by.

*Author to whom all correspondence and reprint requests should be addressed.

INTRODUCTION

To obtain high reaction rates per unit volume of reactor and good flow properties, the industrial insolubilized enzyme catalysts should have a large protein loading and not have a very small size for the porous support particle. Under these conditions, reaction rates are generally controlled by substrate diffusional limitations, which cause the effectiveness factor of the insoluble enzyme to fall down far from one. Therefore, attempts to improve the efficiency of these biocatalysts are of real interest. Perhaps the most promising approach is the preparation of nonuniformly (or heterogeneously) distributed derivatives in which the enzyme is mostly fixed in the outer part of the porous matrix particle—decreasing activity profile (DAP)—because these DAP nonuniformly distributed derivatives are more efficient than the corresponding uniform ones (1–5). For this reason, in the last few years, several reports have appeared in the literature concerning the preparation and kinetic behavior of these nonuniformly distributed insolubilized enzyme derivatives (*1–7*), but in spite of this increasing interest, many basic problems yet remain unanswered.

In this paper we present a study on three different, related aspects of the preparation and kinetic behavior of DAP-nonuniformly distributed insolubilized enzymes:

(1) A simple theoretical model for a process influenced by the substrate diffusion speed and enzymatic reaction rate (mixed enzymic reaction–internal diffusion kinetics) is proposed. With this model we have tried to answer several basic questions: Is there a qualitative influence of DAP distribution on the kinetic behavior of insolubilized enzyme derivatives compared to uniformly distributed ones? Is there a qualitative influence of the specific pattern (linear, in shell, spherical segment and the like) of the DAP distribution? How can DAP distribution, in theory, optimize the efficiency of a certain uniformly distributed enzyme derivative if another derivative could be prepared with the same enzyme concentration per unit volume of support, but distributed nonuniformly?

(2) Using a very common enzyme insolubilization technique (i.e., covalent attachment of enzymes to activated support in a stirred reaction mixture), we have probed the preparation of (DAP) heterogeneously distributed enzyme derivatives. If the insolubilization reaction is performed under enzyme diffusion-controlled conditions (i.e., fast attachment of the protein as compared to its diffusion), and if the

amount of enzyme to be insolubilized is less than the support maximum capacity to bind protein, the enzyme will be mostly insolubilized in the outer part of the porous support particle. Obviously, higher insolubilization rates and/or lower enzyme diffusion rates will yield more heterogeneous enzyme distributions. Intrinsic insolubilization rates will be determined by the reactivity and concentration of active groups in the support, the enzyme concentration, pH temperature, and so on. Enzyme diffusion rates will be influenced by the diffusivity of the enzyme in solution, enzyme concentration, textural properties of the support, and so on.

For this experimental study, the system (CNBr-activated) agarose-micrococcal nuclease has been chosen. In order to obtain large variations in the insolubilization rate/enzyme diffusion rate ratio, which will translate into very different heterogeneous distributions, the following steps have been carried out: (a) Agarose gels with very small pore diameter (similar to the nuclease size) have been prepared, and the protein progress within the pores of these gels must be very restricted; (b) the CNBr activation method yields agarose gels with very high insolubilization rates for NH_2-containing molecules (*8*), and very high concentrations of active groups—cyanates—in the agarose can be readily obtained; (c) the maximum amount of nuclease insolubilized in the agarose beads represents less than 1% of the maximum capacity of the gels; and (d) the presence of internal diffusional limitations during the insolubilization reaction, and the influence of the activation degree of the support in the insolubilization rates, have been experimentally proven.

Under these conditions, one should expect very different enzyme distributions in the derivatives. (The distribution of the protein was quantitatively determined by fluorescence microscopy.) From these experiments, we expected to gain some insights into how difficult it is to obtain very (DAP) nonuniformly distributed, insolubilized enzyme derivatives.

(3) Finally, we have studied the kinetic behavior of agarose-nuclease derivatives in the hydrolysis of thymidine 5′-(*p*-nitrophenyl phosphate)3′-phosphate, synthetic substrate of the nuclease. With these data, our theoretical model was checked. [This same experimental system, but using commercial agarose gels of large pore size as supports, allowed us to verify the usefulness of a similar, simpler model describing the kinetic behavior of uniformly distributed insolubilized enzymes (*9*)].

THEORY

We consider an insoluble enzyme system as having the following properties: (a) The solid support particles are spherical; (b) since the diffusion of the reaction products are larger than that of the substrate, only the diffusion influence of the latter is considered; (c) the intrinsic enzyme kinetics of these insolubilized nuclease derivatives are of the Michaelis-Menten type; (d) the flux of substrate through the porous structure obeys Fick's first law, with a constant effective diffusion coefficient, D_{eff}; (e) there is no external diffusion influence (this point has been proven experimentally); (f) there are no temperature gradients; and (g) the mass transfer takes place under stationary conditions.

As discussed previously for uniformly distributed, insolubilized enzymes (9), in a volume of differential element of insolubilized derivative, at steady state, the difference between the substrate diffusion speed through the surfaces of radii $r + dr$ and r will be equal to the enzymic reaction rate. In a dimensionless form, one can write:

$$\frac{d^2Y}{d\rho^2} + \frac{2}{\rho}\frac{dY}{d\rho} - \phi(\rho)^2\beta\frac{Y}{\beta + Y} = 0 \qquad (1)$$

where

$$Y = S(r)/S_0 \qquad \rho = r/R \qquad \beta = K'_m/S_0$$

and

$$\phi(\rho) = R\left(\frac{E(\rho)\ k'_{cat}}{D_{eff}K'_m}\right)^{1/2} = R\left(\frac{E_M k'_{cat}}{D_{eff}K'_m}\right)^{1/2}\left(\frac{E(\rho)}{E_M}\right)^{1/2}$$

$$= \phi_M\left(\frac{E(\rho)}{E_M}\right)^{1/2} \qquad (2)$$

The boundary conditions for Eq. (1) are:

$$dY/d\rho = 0 \text{ at } \rho = 0$$
$$Y = 1 \quad \text{at } \rho = 1$$

The solution of Eq. (1), $Y = Y(\rho)$, will be determined by the values of β and ϕ_M and by the distribution function of the enzyme in the insoluble derivative. $f(\rho) = E(\rho)/E_M$. Two types of enzyme distribution in the particles were considered:

(a) *Distribution in spherical segment.* The enzyme is bound uniformly only in the external shell of the support particle. An adimensional radius, ρ_c, is considered such as:

$$\begin{aligned} f(\rho) &= 0 \\ \phi(\rho) &= 0 \end{aligned} \qquad \text{where } \rho < \rho_c$$

$$\begin{aligned} f(\rho) &= (1 - \rho_c^3)^{-1} \\ \phi_{sh} &= \phi_M(1 - \rho_c^3)^{-1/2} \end{aligned} \qquad \text{when } \rho \geq \rho_c \tag{3}$$

(b) *Linear distribution.* Starting from the surface of the particle, the concentration of the bound enzyme decreases linearly down to zero for an adimensional radius, ρ_1, such as:

$$f(\rho) = 0 \qquad \text{when } \rho < \rho_1$$

$$f(\rho) = \frac{\rho - \rho_1}{\int_0^1 (\rho - \rho_1)\rho^2 d\rho} \qquad \text{when } \rho \geq \rho_1$$

In order to solve Eq. (1) for both types of enzyme distribution, a computer program applying the fourth-order integration method of Runge-Kutta (*10*) was used.

Effectiveness Factor

One way of calculating the effectiveness factor, η, is to consider that at steady state the actual reaction rate in the whole sphere is equal to the diffusion rate of the substrates through the entire surface toward the inside of the particle. Then

$$\eta = \frac{\text{actual overall reaction rate, } Y = Y}{\text{reaction rate if } Y = 1}$$

$$\eta = \frac{3(\beta + 1)\left(\frac{dY}{d\rho}\right)_{\rho = 1}}{\phi_M^2 \beta} \tag{4}$$

Once we know $Y = Y(\rho)$, by solving Eq. (1), we can calculate $(dy/d\rho)_{\rho = 1}$ and hence also solve Eq. (4). The value of η will be a function of ϕ_M, β, and $f(\rho)$.

Analytical Solutions of Eq. (4)

Shell-Type Distributions

For shell-type heterogeneous enzyme distributions and in the limiting cases of Michaelian kinetics (first and zero order), the simplified Eq. (4) has analytical solutions:

First Order ($\beta \rightarrow \infty$)

Solutions of simplified Eqs. (1) and (4) have been given by Aris (*11*):

$$Y(\rho) = 1/\rho \frac{\phi_{sh}\rho_c \cosh \phi_{sh}(\rho - \rho_c) + \sinh \phi_{sh}(\rho - \rho_c)}{\phi_{sh}\rho_c \cosh \phi_{sh}(1 - \rho_c) + \sinh \phi_{sh}(1 - \rho_c)}$$

and

$$\eta_1 = \frac{3\phi_{sh}(1 - \rho_c)\cosh \phi_{sh}(1 - \rho_c) + \phi_{sh}^2 (1 - \rho_c^3)\phi_{shc}\cosh \phi_{sh}(1 - \rho_c) + (\phi_{sh}^2\rho_c - 1)\sinh \phi_{sh}(1 - \rho_c)}{\sinh \phi_{sh} (1 - \rho_c)} \quad (5)$$

and, since $\phi_{sh} = f(\phi_M, \rho_c)$ [*see* Eq. (3)], then

$$\eta_1 = f' (\phi_M, \rho_c)$$

When $\rho_c = 0$, Eq. (5) becomes the one previously obtained by Wheeler (*12*):

$$\eta_1 = \frac{3}{\phi} \left[\frac{1}{\tanh \phi} - \frac{1}{\phi} \right] \quad (6)$$

which is valid for uniformly distributed derivatives (*9*). $\phi = \phi_M = \phi_{sh}$ is the Thiele modulus of a derivative with uniform enzyme distribution.

Zero Order ($\beta \rightarrow 0$)

We can now apply a reasoning parallel to that we previously used for homogeneously distributed, insolubilized enzymes (*9*). First, we consider an adimensional radius, ρ_{ex}, at which the substrate concentration becomes zero; this radius will be defined by the equaton, obtained by Weekman and Gorring (*13*).

$$\phi_{sh}^2\beta = \frac{3}{(1 - \rho_{ex})^{1/2}(1 + \rho_{ex}) - \rho_{ex}^2} \quad (7)$$

And replacing ϕ_{sh} with its value in Eq. (3), we have

$$\phi_M^2\beta = \frac{3(1 - \rho_c^3)}{(1 - \rho_{ex})^{1/2} (1 + \rho_{ex}) - \rho_{ex}^2} \quad (8)$$

At this point we can consider two situations for shell-type, nonuniformly distributed, insolubilized enzymes:

(A) If $\phi_M^2\beta \leq 3(1 - \rho_{ex})^3/(1 - \rho_{ex})[1/2(1 + \rho_{ex}) - \rho_{ex}^2]$

this means that $\rho_{ex} > \rho_c$ and, thus, the substrate concentration will be finite (>0) in all the shells (spherical segment) containing insolubilized enzyme; hence $\eta_0 = 1$.

$$\text{(B) If } \phi_M\beta > 3(1 - \rho_{ex})^3/(1 - \rho_{ex})[\tfrac{1}{2}(1 + \rho_{ex}) - \rho_{ex}^2]$$

then $\rho_{ex} < \rho_c$, and there will be two different volume fractions in the shell containing the enzyme; (a) where substrate concentration is zero, and (b) where substrate concentrations is finite (>0). The effectiveness factor, η_0, will be the volume fraction of the shell where substrate concentration is finite:

$$\eta_0 = \frac{1 - \rho_{ex}^3}{1 - \rho_c^3} = f(\phi_M, \rho_c, \beta)$$

because ρ_{ex} is defined by Eq. (8).

RESULTS AND CONSIDERATIONS FROM THE THEORETICAL MODEL

From the numerical solutions of Eq. (1) we can obtain the theoretical Eadie-Hofstee plot corresponding to every pair of given values ϕ_M and $f(\rho)$. These Eadie-Hofstee plots had been previously chosen as the most adequate for the study diffusional limitations in reactions catalyzed by insolubilized enzymes (*9*). For this analysis—which considers only the limiting case of internal diffusion–enzymic reactions—the equation that defines the initial rate of reaction per unit volume of insolubilized enzyme particle, v, is:

$$\frac{v}{E_M S_0} = \eta[\phi_M, \beta, f(\rho)]\left[\frac{k'_{cat}}{K'_m} - \frac{v}{K'_m E_M}\right]$$

Figure 1 shows the Eadie-Hofstee theoretical lines for a single value of ϕ_M and different values of ρ_c. We see that when ρ_c increases, the line (sigmoidal) tends to coincide with the straight line corresponding to the soluble enzyme; that is, η increases with ρ_c. One can observe that the lines obtained are very similar for the uniform enzyme distribution and for different pairs of values ϕ_M and ρ_c in the nonuniform distributions. For example, the sigmoidal curve of a nonuniform enzyme derivative of $\phi_M = 10$ and $\rho_c = 0.95$ (Fig. 1), also corresponds to other inhomogeneous derivatives (i.e., $\phi_M = 6.8$ and $\rho_c = 0.9$; $\phi_M = 4$ and $\rho_c = 0.68$, and so on) and also to a uniform enzyme derivative having a value $\phi_M = 3.2$. In addition, the similarity among all these theoretical lines is maintained throughout all β values, even for the region where $\beta \to \infty$.

On the other hand, theoretical representations obtained for different types of enzyme distribution are also quite similar. The theoretical lines

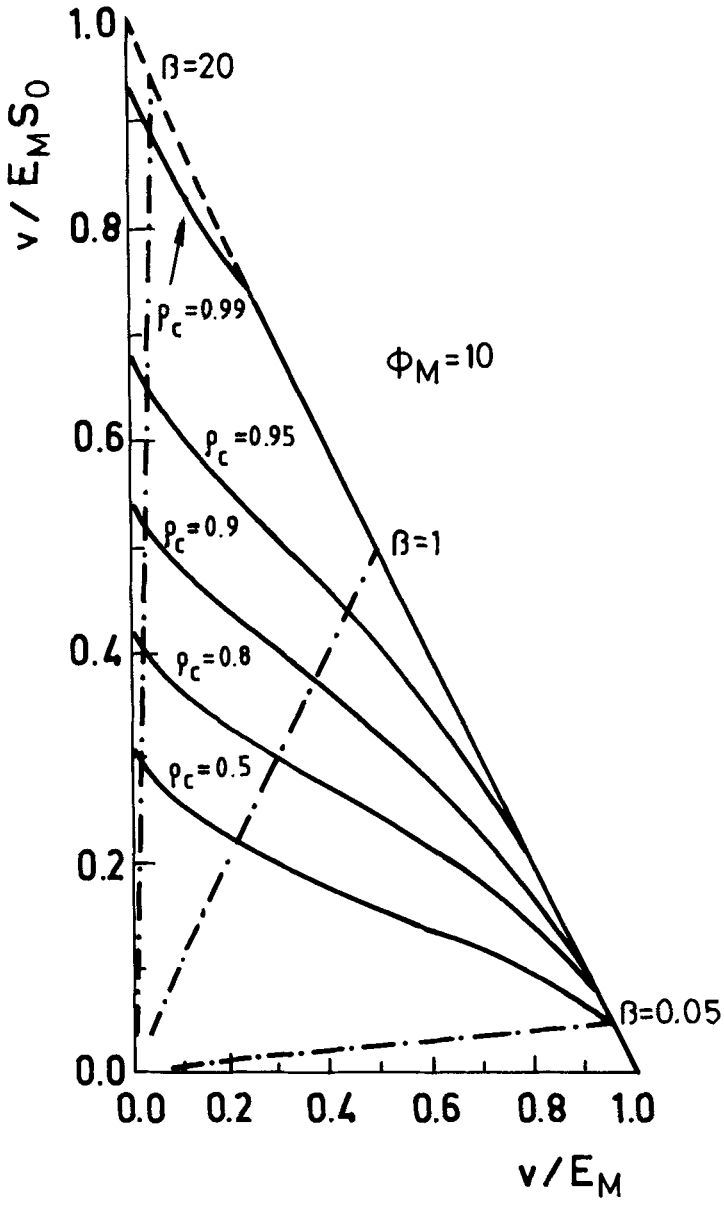

Fig. 1. Theoretical Eadie-Hofstee plots for five nonuniform insolubilized enzyme derivatives with a constant value of ϕ_M (=10) and different ρ_c (solid lines). The following values were used: R = 1 μm; k'_{cat} = 1/s; K'_m = 1 μM; E_M = 1 μM: D_{eff} = 0.01 cm^2/s: The straight line connecting values of 1.0 at the coordinates represents the behavior of a soluble enzyme obeying Michaelian kinetics; the broken lines (· - ·) corresponds to values of β from 20 to 0.05.

corresponding to three values of ϕ_M (7, 15, and 30) are given in Fig. 2. In any case, a single sigmoidal curve is obtained for two derivatives having the same ϕ_M, but a different type of enzyme distribution: (i) a spherical segment of ρ_c = 0.9; or (ii) a linear distribution with ρ_1 = 0.82.

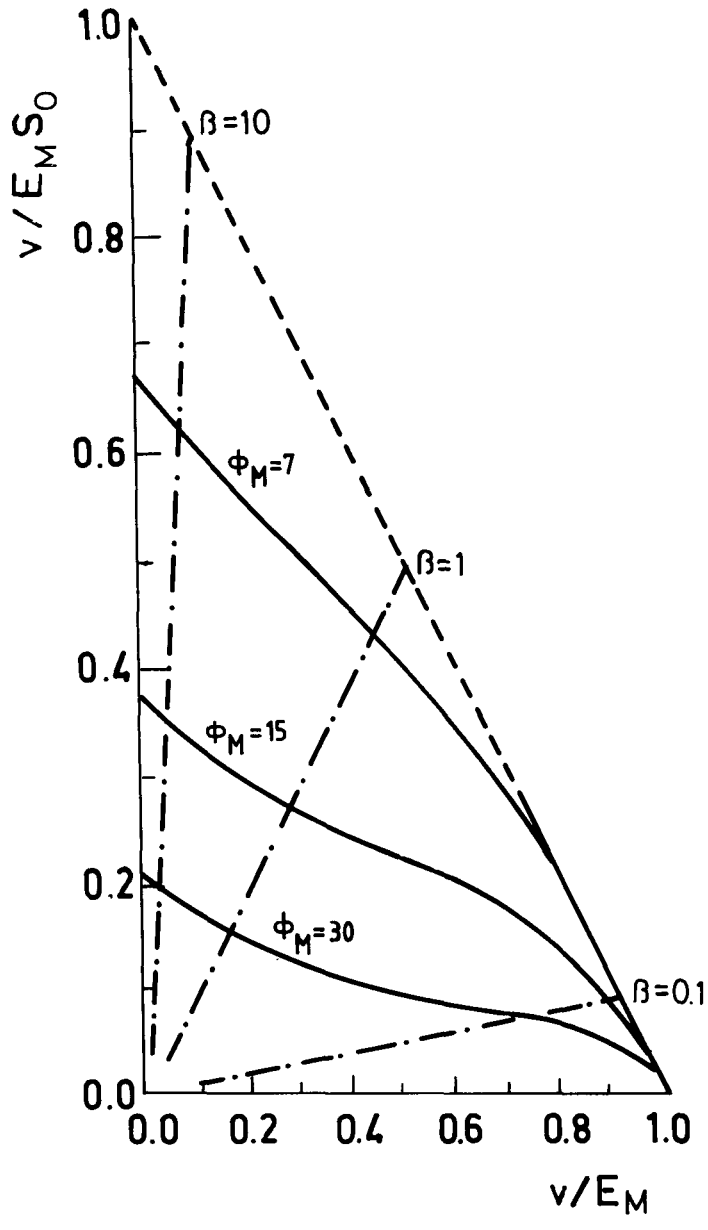

Fig. 2. Theoretical Eadie-Hofstee representations for three insolubilized enzyme derivatives having ϕ_M values of 7, 15, and 30. The same curve is obtained for two derivatives possessing the same ϕ_M, but a distribution in a spherical segment of $\rho_c = 0.9$ or a linear distribution of $\rho_1 = 0.82$. The values of R, K'_{cat}, k'_m, and E_M are as in Fig. 1. The D_{eff} values corresponding to ϕ_M of 7, 15, and 30 are, respectively, 0.02, 0.0044, and 0.0011/ cm^2/s.

Based on these findings, the study of the kinetic behavior of insoluble derivatives having a heterogeneous enzyme distribution can be largely simplified as follows: (a) Whatever the type and pattern of the DAP-heterogeneity in the enzyme distribution may be, its kinetic behav-

ior will be similar to that of a certain derivative with a uniform enzyme distribution (characterized by an apparent Thiele's modulus ϕ_{app}); (b) whatever the pattern of the DAP-heterogeneity in the enzyme distribution may be, its kinetic behavior will be similar to that of a certain derivative having the enzyme distributed in a spherical segment (defined by the value ρ_{eq}). This leads us to the following statement concerning the kinetic behavior of insoluble enzyme derivatives:

Any type and pattern of nonuniform enzyme distribution [characterized by ϕ_M and $f(\rho)$] can be made equivalent to a distribution in spherical segments (defined by ϕ_M and ρ_{eq}) and to a uniform distribution (defined by ϕ_{app}), i.e.,

$$[\beta, \phi_M, f(\rho)] = (\beta, \phi_M, \rho_{eq}) = (\beta, \phi_{app})$$

Following our model and using the numerical solutions of the limiting case $\beta \rightarrow \infty$ (first order), the relationship among ϕ_{app}, ϕ_M, and ρ_{eq} can be readily obtained. For this, we equate the value of η_1 for a uniform derivative with ϕ_{app} [Eq. (6)] to the value for a nonuniform derivative defined by ϕ_M and ρ_{eq} [Eq. (5)]. Thus:

$$\eta_1(\phi_{app}) = \eta_1(\phi_M, \rho_{eq}) \tag{9}$$

Some numerical results of Eq. (9) are presented in Fig. 3.

The fitting of the kinetic experimental data to the theoretical model cannot be done unequivocally. Information on the enzyme distribution in the derivative or on ϕ_M (i.e., information on the nonkinetic parameters that define ϕ_M, i.e., R, E_M, D_{eff}) is needed. To adjust experiment and theory, the following procedure is proposed:

(i) Fit the experimental results (presented as Eadie-Hofstee plots) to the theoretical model, internal diffusion—enzymic reaction, corresponding to insolubilized derivatives with uniform distribution, as has been published previously (9). From this fitting we can obtain k'_{cat}, K'_m, and ϕ_{app}.

(ii) From ϕ_{app} and using the solutions to Eq. (9), the value of ϕ_M (if we previously know ρ_{eq}), or the value of ρ_{eq} (if we know all the parameters that define ϕ_M) can be calculated.

Finally, in order to explore the possibility of optimization of insolubilized enzyme derivatives by means of heterogenization of enzyme distribution, plots of the percentage of effectiveness versus log $(1 - \rho_{eq})$ for different ϕ_M and β values are represented (Fig. 4). At 100%, the effectiveness factor corresponding to the homogeneously distributed derivative for a given value of ϕ_M was taken. As expected, the increase in effectiveness is more pronounced when both ϕ_M and β increase. However, it should be noted that spectacular increases are only obtained for very extreme inhomogeneous distributions. Thus, in the most extreme case represented in Fig. 4 ($\phi_M = 40$, $\beta \rightarrow \infty$), only a 35% increase in the effectiveness factor (with respect to the corresponding homogeneous

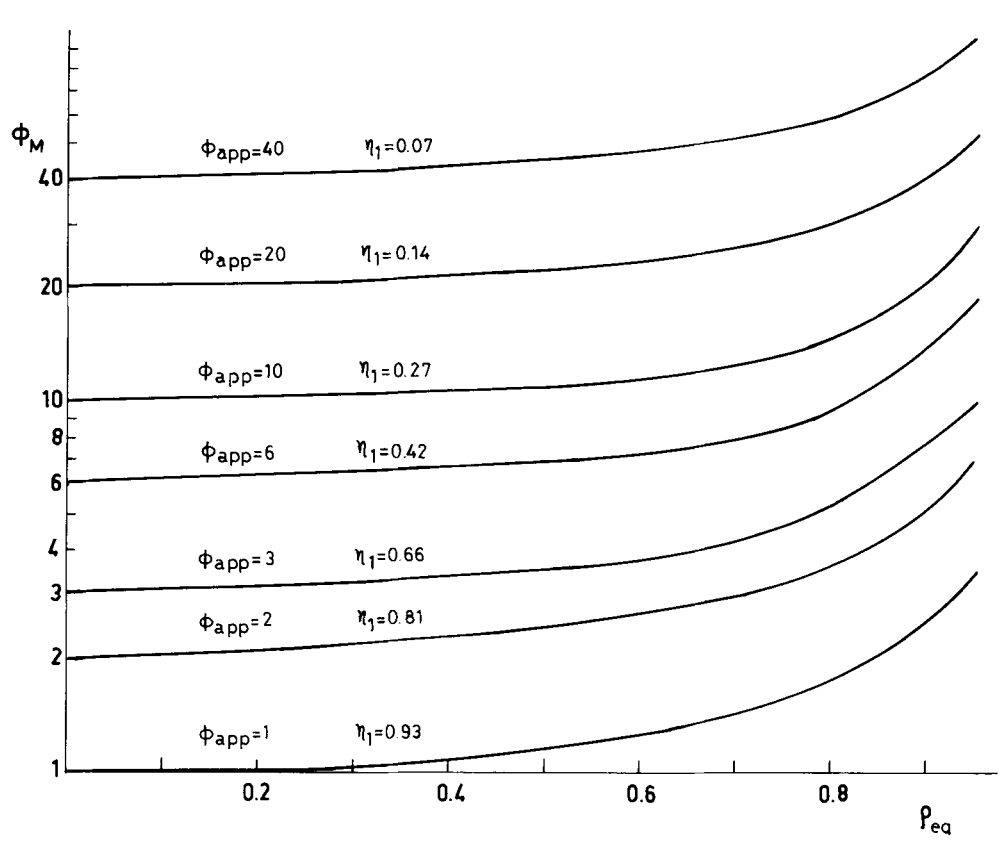

Fig. 3. Some numerical solutions of Eq. (9) showing the kinetic equivalence between ϕ_{app} and different pairs of values (ϕ_M, ρ_{eq}).

derivative) is obtained for a clearly nonuniform distribution ($\rho_{eq} = 0.7$). This point will be further commented on in the Discussion.

EXPERIMENTAL

Materials

Sepharose 2B and 6B were from Pharmacia, Sweden; CNBr from E. Merck, West Germany; micrococcal endonuclease (EC 3.1.31.1.; mw 16.800) from Worthington Biochemical Corporation, USA; and thymidine 5′-(*p*-nitrophenyl phosphate)3′-phosphate (NPpdTp), from Ash Stevens Inc., 5861 John C. Lodge Freeway, Detroit, MI 48202. All other reagents were from commercial sources.

Methods

Preparation of Agarose Gels A26 and A44

The preparation of very dense agarose gels was carried out by treating commercially available gels according to the directions outlined

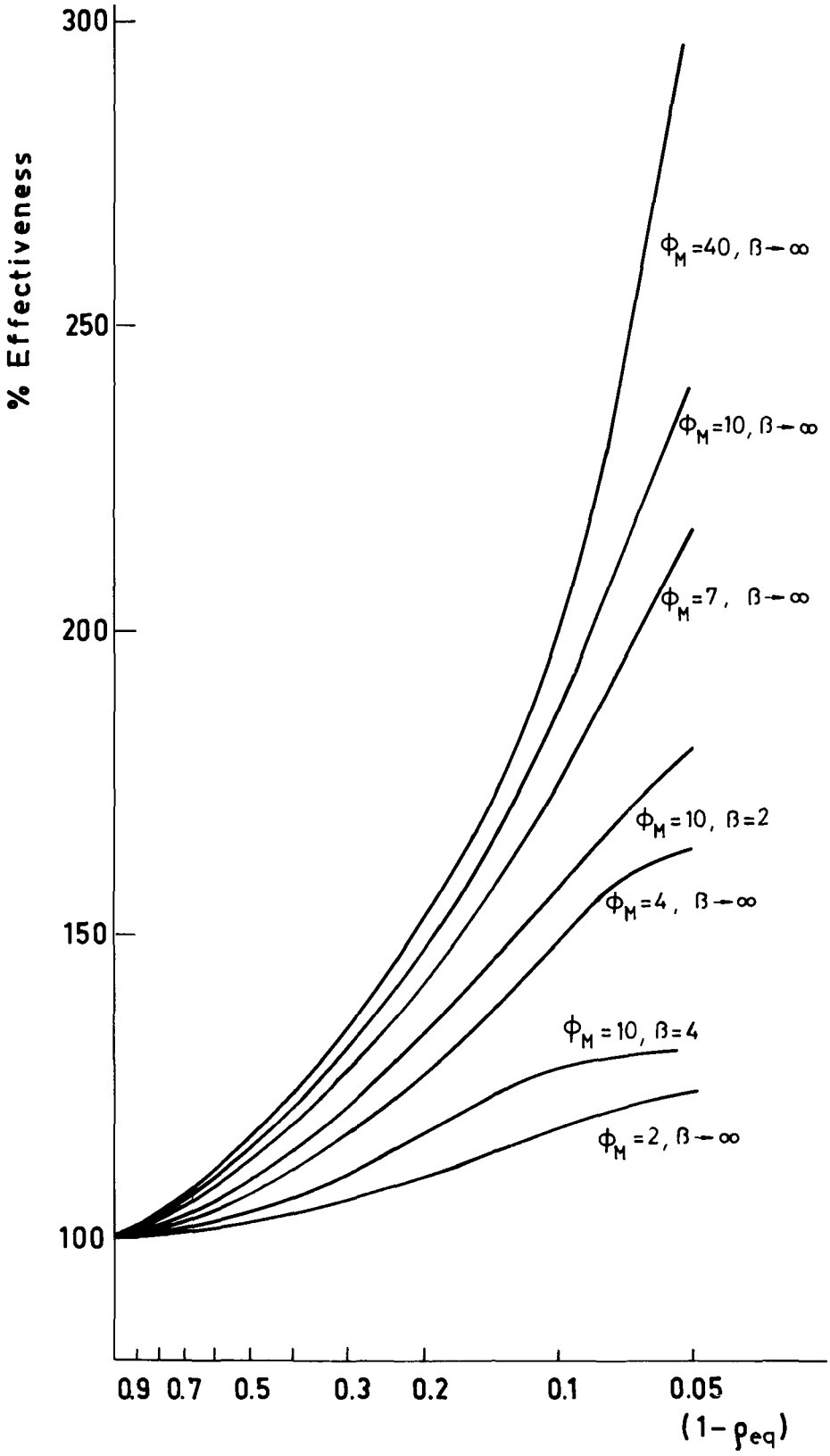

Fig. 4. Theoretical increase of the effectiveness factor for nonuniform distribution of enzyme. Comparison between uniform (% effectiveness = 100) and shell-type distributions with the same E_{M}. (Erratum: the 2nd line from bottom corresponds to $\phi_M = 7$, $\beta = 4$).

by Porath and Axén (*14*). An agarose gel containing 6% (w/v) agarose (Sepharose 6B, from Pharmacia) was dehydrated by successive washings with ethanol–water mixtures of decreasing water content and, finally, with absolute ethanol. To avoid lump formation, the gel was then mildly dried in a desiccator (24 h at room temperature and 2 h *in vacuo*). One gram of the dried agarose was swollen in 45 mL of the ethanol–water mixture (20: 80 for A26 and 37:63 for A44) containing 0.5*M* NaCl and 5 mg/mL $NaBH_4$. The swelling was affected at 60°C for 5 min; then 3.8 mL epichlorohydrin/g dried powder were added and the mixture left for 2 h in order to fix the new tridimensional structure of the gels. Then they were washed, heated in an autoclave, and washed again as recommended by Porath and Axén (*14*). The gels so obtained contained 13 and 20% (w/v) agarose, respectively. Their activation with CNBr (*see* procedure below) apparently rendered their porous structures closer together, since the activated gels—A26 and A44—now contained 26 and 44% agarose (w/v), respectively.

CNBr Activation

Activation with CNBr was carried out according to the latter method of Porath et al. [procedure A of ref (*15*)], which takes advantage of the very high buffer capacity of alkaline phosphate solutions, rendering pH control unnecessary. In the standard procedure, 150 mg of CNBr/mL gel were used. The determination of active cyanate groups, the main groups responsible for enzyme binding, was made using the procedure of Kohn and Wilchek (*8*). As pointed out above, the CNBr activation affects the porous structure of the modified gels. Thus, in order to have very different activation degrees, we did not use different conditions in the activation procedure, but the gels were activated by the standard procedure (150 mg BrCN/mL gel), and in some cases they were allowed to deactivate in 0.1*M* $NaHCO_3$ buffer, pH 9.0, until the desired activation degree (measured as concentration of cyanate groups) had been reached.

Textural Characterization of the Gels

This was made by using optical microscopy, gel filtration, and solute partitioning equilibrium (*16*). The gels were characterized by their particle radius, pore diameter, and specific area. Details will be give elsewhere (J. M. Guisán and J. Serrano, in preparation). Gels A26 and A44 were studied after CNBr activation. After activation they were deactivated in 0.1*M* $NaHCO_3$, pH 9.0; and for blockage of the residual active groups they were treated overnight with 1*M* ethanolamine, pH 9.0.

Values of textural parameters for two commercial Sepharoses and for the dense agarose gels (A26 and A44) are presented in Table 1. The pore diameter of the commercial Sepharose 6B was reduced by more than an order of magnitude down to the range of the nuclease size, $3 \times 3 \times 4$ nm (*17*).

TABLE 1
Properties of the Supports

	2B	6B	A26	A44
d_p, nm	250	80	7	5
R, μm	50	50	38	27
a_{sp}, m^2/cm^3	8	25	130	185

Preparation of Insolubilized Derivatives

Nuclease was insolubilized through its amino groups directly on the BrCN activated agarose, essentially as previously reported (*18*). Insolubilization was carried out in 0.1*M* bicarbonate buffer and 0.5*M* ClNa, pH 9.0, at room temperature. Typical insolubilization mixtures (amount of enzyme/amount of activated gel/total vol) are detailed in the legend of Fig. 5. The amount of enzyme insolubilized was obtained from the difference between the activity of the soluble enzyme added to the insolubilization mixture and the activity recovered in the filtrate and washings. In control experiments with unactivated agarose, the activity of the enzyme in the filtrate and washings remained at 100%.

Enzyme Assays

Initial activity of the soluble and insoluble enzymes toward NPpdTp was measured by following graphically the increase in absorbance at 330 nm at 25°C (*19*), using a Zeiss PMQII spectrophotometer equipped with a 2-cm pathlength cuvet, with magnetic stirrer. The stirrer speed, determined with a tachometer, was usually fixed at its maxima setting (2500 rpm). Reaction velocities were calculated using a molar extinction coefficient for the *p*-nitrophenyl phosphate at 330 nm of 4260/*M*/cm (*19*). Measurements of activity were made at pH 9.5 (50 m*M* glycine–NaOH buffer). The amount of insolubilized derivative in the assays was always maintained in the region of linearity between activity and amount of derivative. Hence, the ratio between the observed reaction rate and the volume of insolubilized enzyme present in the reaction (i.e., in the spectrophotometer cuvet) gives the actual reaction rate per unit volume of enzyme derivative, v.

Determination of Enzyme Distribution

Agarose-nuclease derivatives were suspended for 1h at room temperature in a 40-μg/mL fluorescein isothiocyanate solution in 0.1*M* $NaHCO_3$, pH 8.5. Afterward, the gel was exhaustively rinsed, as described previously (*18*), then inbedded in 20% (w/v) gelatine and cut into 5-μm sections, following the procedure of Lasch et al. (*20*). These sections were analyzed with a scanning Zeiss fluorescence microscope, model SMPH. The intensity of fluorescence present in the 5-μm thick-

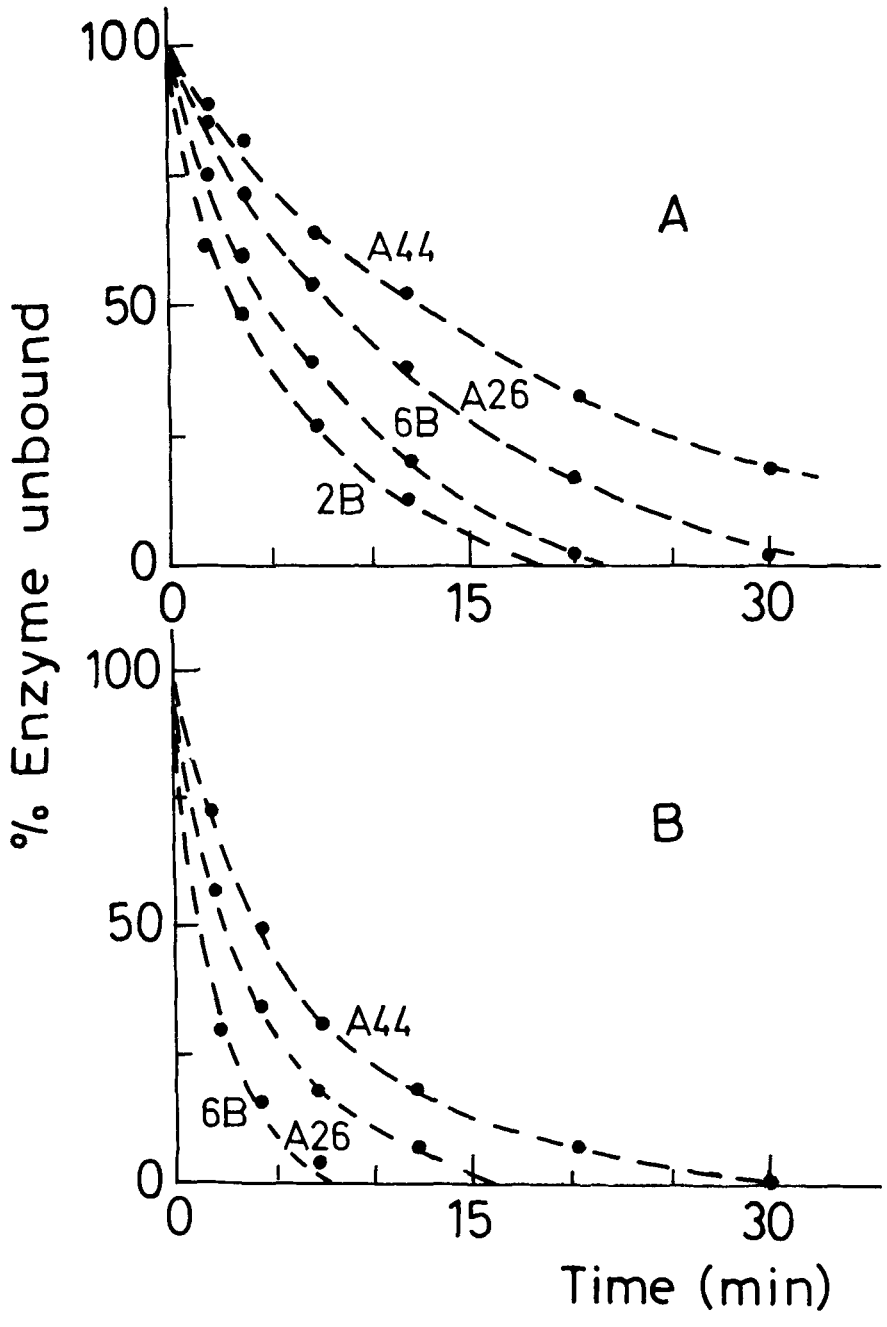

Fig. 5. Insolubilization of nuclease on CNBr-activated agarose gels. The reaction conditions were the following: Gel volume, 2 mL; total reaction volume, 25 mL; and enzyme concentration, 13.4 μg/mL. Activation degree of the gels: (A) 3.3 m*M*; and (B) 7.7 m*M* in cyanate groups.

ness of a bead section when scanned along a diameter, was measured with the help of a computer.

RESULTS

Influence of the Nuclease Diffusion During the Insolubilization Reaction

The speed of the insolubilization reaction has been studied by varying the porous structure of the support while keeping the remaining variables (concentration of cyanate groups in the support, enzyme concentration in the insolubilization mixture, temperature, and so on) constant. Figure 5 shows a time course of the immobilization of nuclease on several agarose gels at two different activation degrees of the supports. In both cases, the time required for insolubilization is higher the lower the pore diameter of the support. Likewise, the reaction time decreases for increasing support activation (concentration of cyanate groups, *see* Table 2). Lower times for the insolubilization reaction result in nonuniform distribution (*21*), with the enzyme mostly bound in the external part of the beads. We have chosen this procedure, the variation in the activation degree of the support, as a way of obtaining several different insolubilized derivatives, all having the same average concentration of enzyme, E_M, but very different protein distribution.

The properties of pairs of derivatives having the same enzyme concentration, but differing by one order of magnitude in the activation degree of the support employed in their preparation, are compared in Table 2. When an enzyme to be covalently insolubilized has many residues that are able to react with the activated support [the nuclease has 24 amino groups (*17*)], an increase in the degree of support activation can favor insolubilization by multiple-point attachment; this multipoint binding could yield derivatives whose intrinsic kinetic properties are very different from those of derivatives having a single-bond enzyme support. From the values of specific surface area (Table 1) and the [NCO^-] (Table 2), the density of cyanate groups on the surface (internal and external) can be calculated. The surface density, expressed as no. of cyanates/1000 $Å^2$—1000 $Å^2$ is approximately the section occupied by a molecule of

TABLE 2
Properties of the Insolubilized Derivatives

	N-A26n	N-A26u	N-A44n1	N-A44u1	N-A44n2	N-A44u2
E_M, μM	10	10	17.5	17.5	9.0	9.0
[NCO^-], mM	11	1.1	13	1.1	13	1.1
Surface density[a]	0.51	0.051	0.42	0.036	0.42	0.036
ρ_{eq}(flu)	0.55	0	0.55	0	0.65	0
ϕ_{app}	14	16	22	25	12	15.5
ϕ_M	16	16	25	25	15.5	15.5
ρ_{eq}(kin)	0.6	0	0.5	0	0.7	0

[a]Expressed as no. cyanate groups/10 nm^2 of support surface.

nuclease—is given in Table 2. In all cases, the surface density is lower than 1; this indicates that in cases of both high and low support activation, the enzyme can be bound only through a single bond. In other words, the range of support activation that is being compared affects only to the protein distribution within the porous structure of the matrix, but not to the intrinsic kinetic properties of the insolubilized enzyme.

Enzyme Distribution in the Derivatives

Quantitative fluorescence analysis of sections of insoluble enzyme particles has been carried out, as described in Methods. As an example, the fluorescence intensity profiles of beads of approximately 70 μm diameter, corresponding to derivaties N-A44u2 and N-A44n2, are presented in Fig. 6. For the insoluble enzyme obtained using the support with the lower activation (N-A44n2), the fluorescence intensity along a diameter remained constant (i.e., the distribution of the enzyme is practically uniform in the gel bead), whereas the more activated support yields a particle of insolubilized enzyme having this bound only in the most external spherical segment. This corresponds to a ρ_c value of 0.7 [*see* the enzyme distribution for other derivatives studied, ρ_{eq} (flu), in Table 2].

Kinetic Studies

First, by varying the stirrer speed, we verified that reaction rates were in all cases independent of the agitation speed in the reactor, i.e., the observed rates of reaction were not influenced by external diffusion.

The substrate concentration was varied between 40 and 220 μ*M*; then pairs of insoluble derivatives having the same support, ϕ_M, and concentration of enzyme in the gel, but different enzyme distribution (practically uniform in one case, *see* Fig. 6A, and clearly nonuniform in the other as Fig. 6B) were compared. Eadie-Hostee plots corresponding to derivatives obtained using the supports of lower porosity are shown in Fig. 7. The points represent experimental values and the lines the theoretical curves predicted by our model. As expected, in all cases, the reaction rate of the derivative with nonuniform distribution of enzyme were always higher than those corresponding to its uniformly distributed counterparts. Furthermore, if we compare derivatives with the same support, but different enzyme concentration, the ordinate values are always higher for the derivative with a lower enzyme concentration (cf N-A44u1 and N-A44u2). That lower concentration of the enzyme in the gel particles yields more efficient derivatives was also found in previous studies (*9*, *18*).

Because of the low porosity of the supports, the deviation of the experimental points from the straight line corresponding to intrinsic insolubilized enzyme kinetics is very large. In a previous work (*9*) we found that when there is no diffusional limitations, the corresponding straight line intersects the ordinate axis at 0.72 and the abcissa axis at 41. The

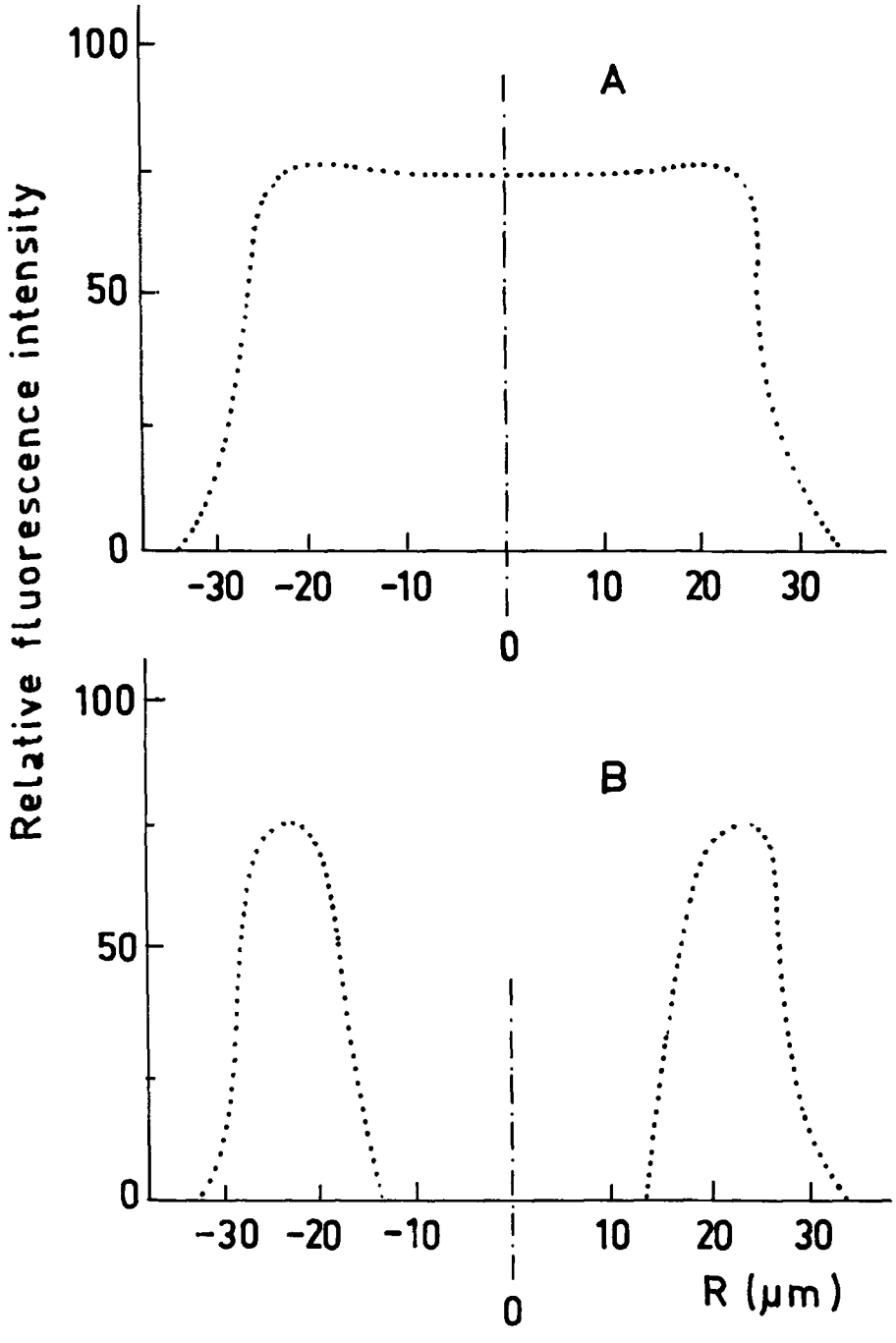

Fig. 6. Quantitative profile of the fluorescence intensity of 5-μm sections of Agarose-nuclease beads of approximately 70 μm in diameter. (A) derivative N-A44u2; and (B) derivative N-A44n2.

large deviations found in the present work indicate serious diffusional resistances, that is, very low effectiveness factors.

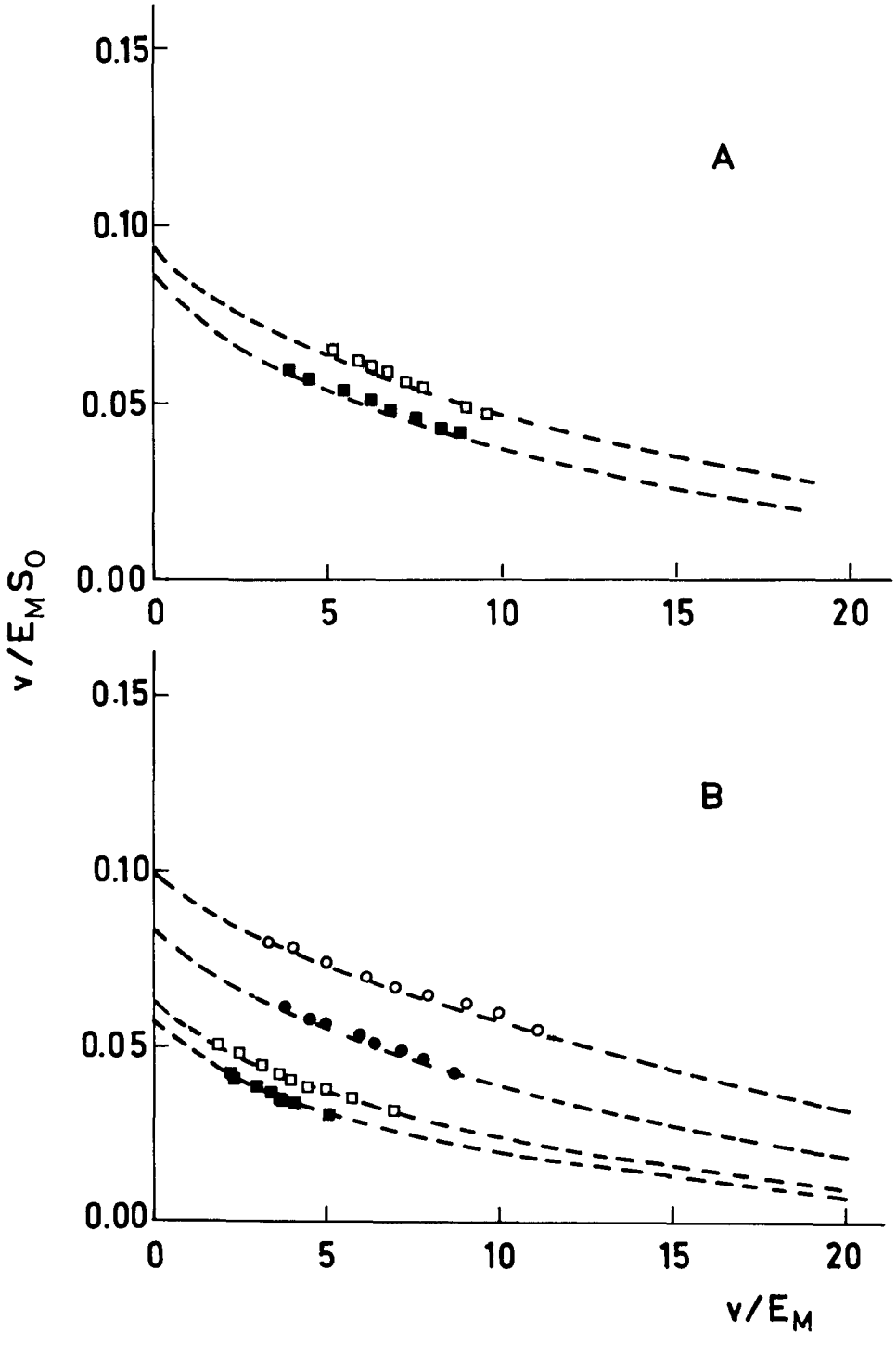

Fig. 7. Eadie-Hofstee plots for three pairs of insolubilized derivatives. The points are experimental values; the lines, the curves according to the theoretical model. Part A: (■) N-A26u; and (□) N-A26n; part B: (●) N-A44u2; (○) N-A44n2; (■) N-A44u1; and (□) N-A44n1.

DISCUSSION

The results depicted in Fig. 5 clearly show the influence of enzyme diffusion in the insolubilization rates. The only difference among the curves of Fig. 5A or B comes from the porosity of the support used, all the other variables being identical; in the absence of diffusonal restrictions, a single curve would be obtained for Fig. 5A and B. Those diffusional restrictions increase when the diffusivity of the enzyme is lower because of a smaller pore diameter of the support. On the other hand, an increase in the concentration of active cyanate groups in the support results in a lower time of insolubilization.

The translation of the diffusional limitations into different enzyme distribution profiles is an expected result, as pointed out in the Introduction. In all cases studied, the concentration of the enzyme in the gel particles was several orders of magnitude lower than the maximal theoretical capacity of the supports (i.e., the concentration of the active cyanate groups, *see* Table 2). In cases of derivatives with nonuniform enzyme distribution (derivatives N-A26n, N-A44n1, and N-A44n2), the enzyme profiles measured followed a clearly cut spherical segment, as indicated by the ρ_{eq}(flu) values listed in Table 2.

The fitting of the experimental data to the theoretical model is simple and can be effected by following steps (i) and (ii), as described in the Theory section. The kinetic behavior of two insolublized derivatives with the same enzyme concentration/mL of gel was compared in all cases; each pair of derivatives compared had the same ϕ_{M1} value, one component had a uniform distribution of the enzyme, the other a nonuniform one. Thus, the ϕ_{app} value obtained for the uniform derivative after applying step (i) is, in fact, the ϕ_{M1} value for both derivatives in the pair. To know the ϕ_{app} from the fitting described in (i), the available information on the intrinsic kinetic constants of this type of derivatives (CNBr-activated agarose-Nuclease, in which the protein was also bound through a single covalent bond) can be used. These constants, which were obtained with a Sepharose 2B-Nuclease derivative (0.1 cyanate/1000 Å^2 of support surface) in the absence of diffusional limitations (*16*), were k'_{cat} = 27.5/min and K'_m = 65 μM. With these data, ϕ_{app}, in the Eadie-Hofstee curve corresponding to each derivative, can be calculated, as previously described (*9*). That is, one has only to extrapolate to the ordinate axis the curve that best fits the experimental points, bearing in mind that the last part of the curve tends to be a straight line parallel to that corresponding to enzymic kinetics. The intersection point will be $\eta_I \phi_{app} k'_{cat}/K'_m$; then, once η_I is known, ϕ_{app} can be calculated from Eq. (8). The theoretical sigmoidal curve corresponding to this ϕ_{app} value must be contrasted with the experimental one in order to obtain the best possible fitting (this operation may require several extrapolations to the ordinate axis).

Hence, ϕ_{app} values for the nonuniform and uniform derivaties (the latter will be the value of ϕ_{M1} corresponding to both derivatives) for each pair of immoblized derivatives studied can be obtained from kinetic data. Once ϕ_{app} and ϕ_{M1} are known, from Eq. (9) we can obtain the value of ρ_{eq} derived from kinetic measurements, ρ_{eq} (kin). Table 2 presents the value of ρ_{eq}(kin) for three pairs of derivatives compared.

Since the enzyme distribution has been studied by fluorescence microscopy (Fig. 7), which directly gives us the value of ρ_{eq}(flu), the validity of our kinetic model in the conditions of experimentation can be verified. Table 2 clearly shows a very good agreement between ρ_{eq}(flu) and ρ_{eq}(kin).

CONCLUDING REMARKS

From the analysis of the theoretical model developed, we have been able to establish an equivalence in the overall kinetic behavior of insoluble derivatives presenting any type of heterogeneous enzyme distribution, a shell-type heterogeneous distribution, and a uniform distribution. This equivalence allows a great simplification in the kinetic study of DAP-nonuniformly distributed derivatives, as we have seen above. Knowing ϕ_{M1}, and using the theoretical model for uniformly distributed derivatives (9), the value of ρ_{eq}(kin) can be obtained from the analytical solutions of Eq. (9).

Likewise, the model permits *a priori* simulations on the possibilities of optimizing the efficiency of uniform insoluble enzyme derivatives through heterogeneization of the enzyme bound to the porous carrier. From Fig. 4 can be concluded that nonuniform enzyme distributions do not produce dramatic increases in the effectiveness factor of the derivative. For a value of $\rho_{eq} = 0.7$, the highest obtained in our derivatives (Table 2), the increase in the effectiveness factor, even for a system with $\phi_{M1} = 40$, is only 35% (Fig. 4). Experimentally, by preparing a nonuniform derivative of $\rho_{eq} = 0.7$, we have been able to optimize only by 16% a uniform derivative of $\phi_{M1} = 17.6$; $\beta \rightarrow \infty$. On the other hand, we can compare (Fig. 3) the optimization reached by heterogenizing the enzyme distribution with that attained by what is a common technique in catalysis (particle size reduction). In Fig. 3 we see that a uniform derivative ($\rho_{eq} = 0$) of $\phi_{M1} = 30$ can be optimized to the same extent by reducing only threefold its particle size (to $\phi_{M1} = 10$) than by nonuniformly distributing its enzyme up to a $\rho_{eq} = 0.95$.

In the present study the maximum heterogeneization reached has been $\rho_{eq} = 0.7$. This has been obtained by using a low porosity of the support in the insolubilization reaction conditions, an activation method that gives high insolubilization rates and low enzyme loading that favor very unhomogeneous enzyme distributions, but that are far from the

conditions usual in the preparation of insolubilized enzymes on an industrial scale. Therefore, more research is needed to improve the strategies (for example, much larger size of the support particles) to obtain more extremely heterogeneized, insoluble enzyme derivatives.

NOMENCLATURE

a_{sp} Specific surface area (m^2/cm^3).
D_{eff} Effective diffusion coefficiente of substrate (cm^2/s).
d_p Average pore diameter (nm).
E_M Amount of enzyme insolublized per unit volume of derivative: average concentration corresponding to a uniform distribution (μM).
$E(r)$ Enzyme concentration inside the derivative at a distance r from the center of the particle (μM).
$E(\rho)$ Enzyme concentration at an adimensional distance ρ from the center of the particle (μM).
$f(\rho)$ $E(\rho)/E_M$. Adimensional enzyme distribution function in the derivative.
k'_{cat} Intrinsic catalytic constant for the insolubilized enzyme (min^{-1}).
K'_m Intrinsic Michaelis constant for the insolubilized enzyme (μM).
r Distance from the center of the particle (μm).
R Particle radius (μm).
S_0 Substrate concentration in bulk solution (μM).
$S(r)$ Substrate concentration inide the derivative at a distance r from the center of the particle (μM).
v Actual reaction rate per unit volume in an insolubilized derivative (μM/min).
Y $S(r)/S_0$.
ρ K'_m/S_0
ϕ $R(k'_{cat}E/K'_mD_{eff})^{1/}$ 22. General formulation of Thiele modulus in mixed enzymic reaction–internal diffusion kinetics.
ϕ_M $R(k'_{cat} \cdot E_M/K'_mD_{eff})$ $21^{/2}$. Thiele modulus corresponding to an insolubilized derivative in which the enzyme is homogenously distributed.
$\phi(\rho)$ $R(k'_{cat} \cdot E(\rho)/K'_mD_{eff})$s058u21$^{/2}$
ϕ_{Sh} $\phi_M(1 - \rho_c^3)^{-1/2}$. Thiele modulus corresponding to a distribution of enzyme in a spherical segment
ϕ_{app} of a heterogeneously distributed derivative is the Thiele modulus corresponding to an uniformly distributed derivative, which has the same kinetic behavior.
η Effectiveness factor.

$\eta_1\eta_0$ Effectiveness factors corresponding to the limiting cases of first and zero order for enzymic kinetics.

ρ r/R Adimensional distance from center of particle.

$\rho_c = \rho_{sh}$ Adimensional distance for which there is no enzyme, in a particle of shell-type nonuniform derivative.

ρ_1 Adimensional distance for which there is no enzyme, in a linearly distributed derivative.

ρ_{eq} ρ_c equivalent of nonuniformly insolubilized enzyme, whatever be the type of distribution.

$\rho_{eq}(kin)$ ρ_{eq} obtained from the fitting of experimental kinetic data to the theoretical model.

$\rho_{eq}(flu)$ ρ_c obtained from scanning fluorescence microscopy.

ACKNOWLEDGMENTS

We would like to thank Dr. M. L. Bentura, of the CSIC Instituto Cajal, for her collaboration with the fluorescence microscope experiments. The expert technical assistance of M. C. Ceinos is also acknowledged. This research has been supported by the Spanish CAICYT, the Fondo de Investigaciones Sanitarias de la Seguridad Social, and a Fellowship of the Caja de Ahorros and Monte de Piedad de Madrid (to J. S.).

REFERENCES

1. Borchert, A., and Buchholz, K. (1979), *Biotechnol. Lett.* **1,** 15.
2. Buchholz, K. (1979), *Biotechnol. Lett.* **1,** 451.
3. Guisán, J. M., Fernández, V. M., and Ballesteros, A. (1980), Distribution of Staphylococcal Nuclease Insolubilized on Sepharose, in *Enzyme Engineering*, vol. 5, Weetall, H. H., and Royer, G. P., eds., Plenum, New York, NY, pp. 435–438.
4. Buchholz, K., Borchert, A., and Duggal, S. K. (1980), Adsorption of Enzymes in Carriers, in *Enzyme Engineering*, vol. 5, Weetall, H. H., and Royer, G. P., eds., Plenum, New York, NY, pp. 465–468.
5. Park, S. H., Lee, S. B., and Ryu, D. D. Y. (1981), *Biotechnol. Bioeng.* **23,** 2591.
6. Juang, H.-D., and Weng, H.-S. (1984) *Biotechnol. Bioeng.* **26,** 623.
7. Borchert, A., and Buchholz, K. (1984) *Biotechnol. Bioeng.* **26,** 727.
8. Kohn, J., and Wilchek, M. (1981), *Anal. Biochem.* **115,** 375.
9. Guisán, J. M., Melo, F. V. and Ballesteros, A. (1981), *Appl. Biochem. Biotechnol.* **6,** 37.
10. Franks, R. G. E. (1972), *Modeling and Simulation in Chemical Engineering*, John Wiley and Sons, New York, NY.
11. Aris, R. (1971), *Mathematica Theory of Diffusion and Reaction in Permeable Catalysts*, vol. 1, Clarendon, Oxford.
12. Wheeler, A. (1951), *Adv. Catal.* **3,** 249.
13. Weekman, V. W., and Gorring, R. L. (1965), *J. Catalysis* **4,** 260–270. vol. 44, Mosbach, K., ed. Academic, New York, NY, pp. 19–45.
14. Porath, J., and Axén, R. (1976), Immobilization of Enzymes to Agar, Agarose and Sephadex Supports, in *Methods in Enzymology,*

15. Porath, J., Aspberg, K., Drevin, H., and Axén, R. J. (1973), *J. Chromatog.* **86,** 53.
16. Serrano, J. (1981), *Ph. D. Thesis,* Autonomous University of Madrid, Spain.
17. Anfinsen, C. B., Cuatrecasas, P., and Taniuchi, H. (1971), Staphylococcal Nuclease, Chemical Properties and Catalysis, in *The Enzymes,* vol. 4, Boyer, P. D., ed., Academic, New York, NY, pp. 177–204.
18. Guisán, J. M., and Ballesteros, A. (1979), *J. Solid Phase Biochem.* **4,** 245.
19. Cuatrecasas, P., Wilchek, M., and Anfinsen, C. B. (1969), *Biochemistry* **8,** 2277.
20. Lash, J., Iwig, M., and Koelsch, R. (1971), *Eur. J. Biochem.* **27,** 431.
21. Ballesteros, A., Guisán, J.M., and Serrano, J. (1982), Influence of the Activation Degree of the Support on the Properties of Agarose-Nuclease, in *Enzyme Engineering,* vol. 6, Chibata, I., Fukui, A., and Wingard, L. B., Jr., eds., Plenum, New York, NY, pp. 223–224.
3, 313.